Nitrogen-Doped Carbon Encapsulated SnO_2-SnS/Graphene Sheets with Improved Anodic Performance in Lithium Ion Battery

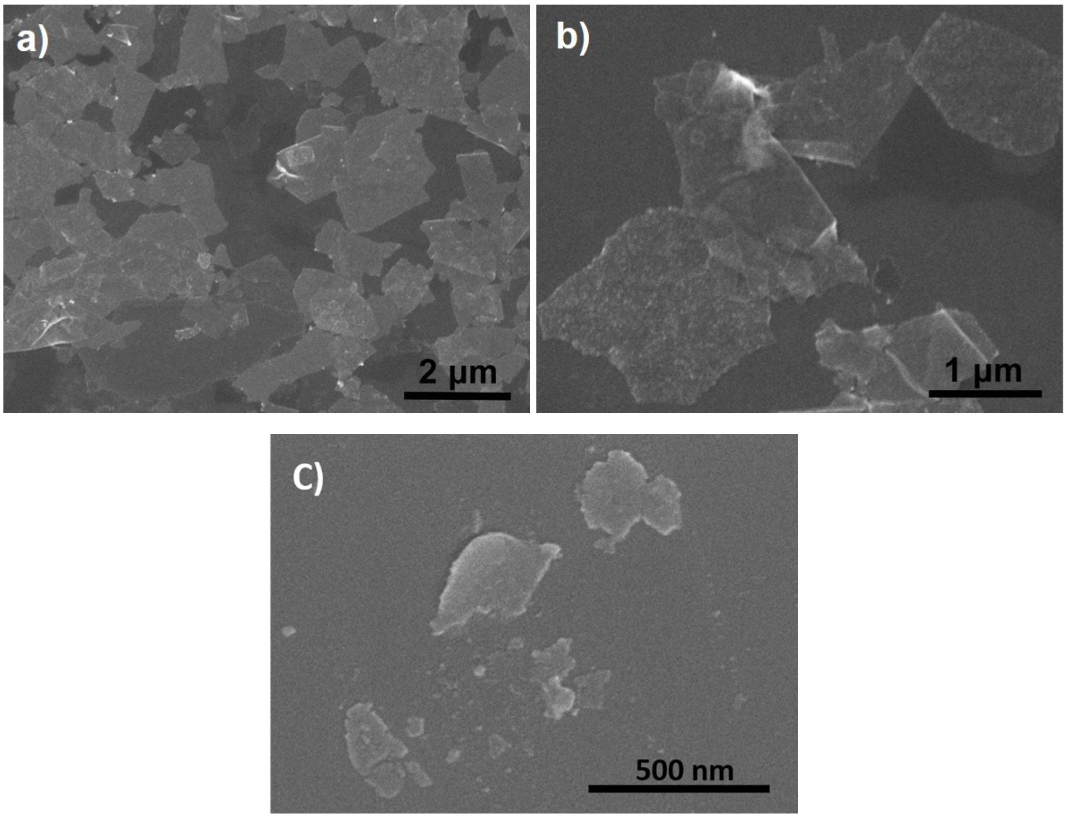

Fig. S1 SEM images of a) C@SnO_2/GN, b) SnO_2/GN and c) N-C@SnO_2-SnS/GN.

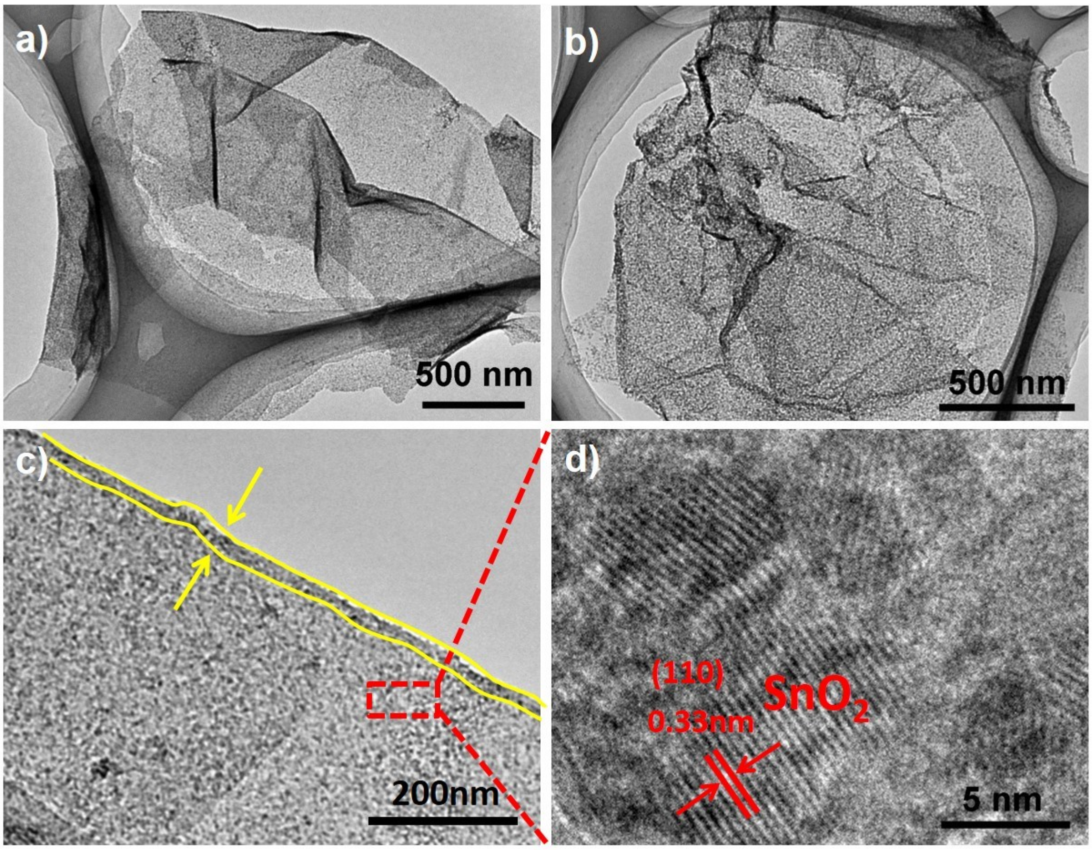

Fig. S2 TEM images of a) and c) C@SnO_2/GN, b) SnO_2/GN, and d) HRTEM image of C@SnO_2/GN.

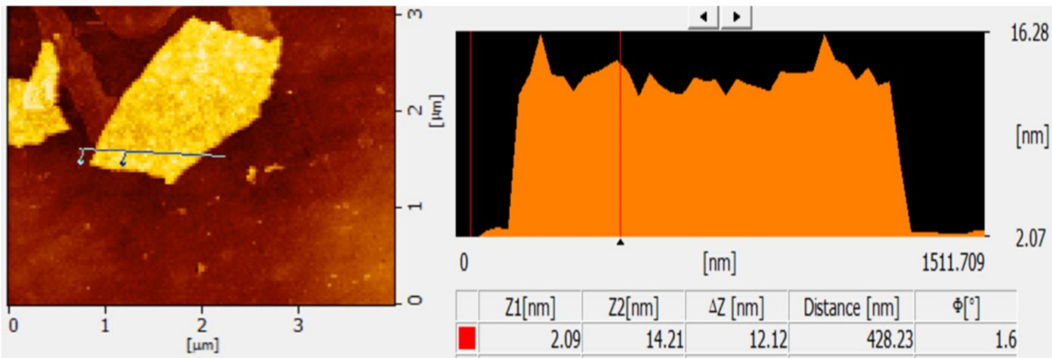

Fig. S3 AFM image of SnO_2/GN.

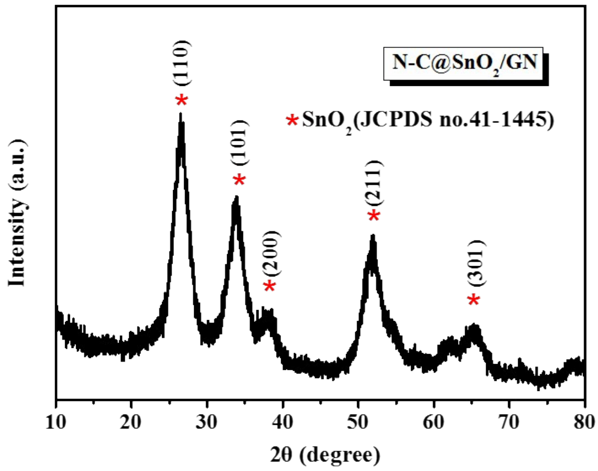

Fig. S4 XRD pattern of N-C@SnO_2/GN.

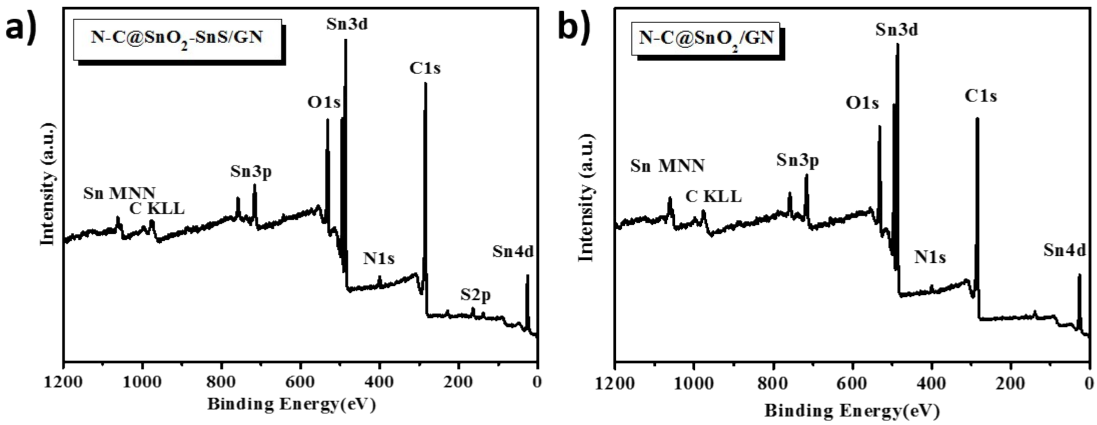

Fig. S5 XPS survey spectra of a) N-C@SnO_2-SnS/GN and b) N-C@SnO_2/GN.

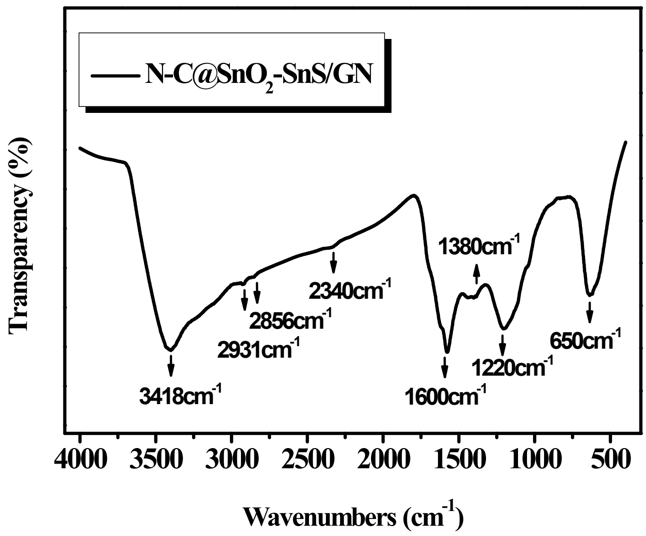

Fig. S6 FTIR spectra of N-C@SnO_2-SnS/GN.

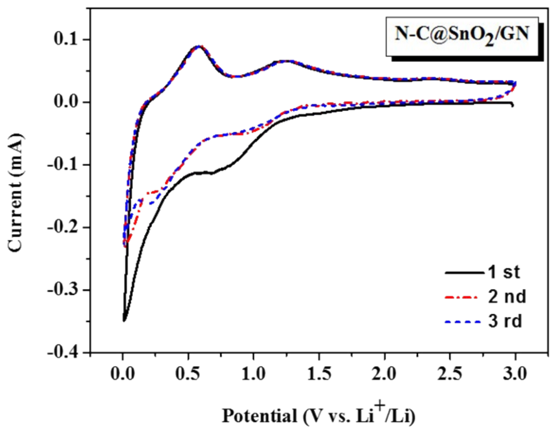

Fig. S7 Cyclic voltammogram (CV) curves of N-C@SnO_2/GN electrode at a scanning rate of 0.1 mV s^{-1} in the voltage range of 0.01 - 3 V vs. Li^+/Li.

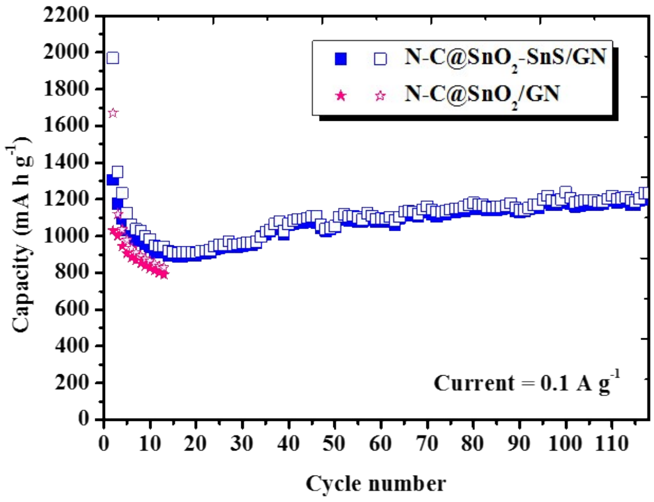

Fig. S8 Cycling performance of N-C@SnO_2/GN and N-C@SnO_2-SnS/GN electrodes in the voltage range of 0.01 - 3 V vs. Li^+/Li.

As shown in Fig. S8, the cycling performance of N-C@SnO_2/GN electrode was evaluated and compared with N-C@SnO_2-SnS/GN. N-C@SnO_2-SnS/GN and N-C@SnO_2/GN delivered initial discharge capacities of 1970 and 1670 mA h g^{-1} at a current density of 0.1 A g^{-1}. After twelve discharge/charge cycles, the corresponding capacities fell to 943 and 828 mA h g^{-1}, respectively. The higher specific capacity and better cycling stability of N-C@SnO_2-SnS/GN provides forceful confirmation to the cushioning effect of SnS in N-C@SnO_2-SnS/GN.

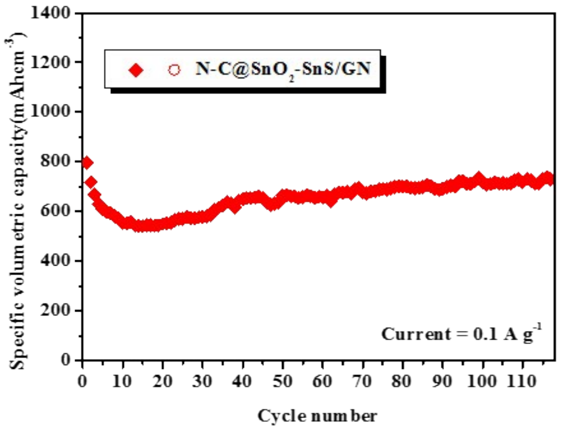

Fig. S9 Specific volumetric capacity vs. cycle number for N-C@SnO2-SnS/GN electrode.

To evaluate the specific volumetric capacity of the sample, we gauged the density of the electrode material composite.[S1] The measured electrode density is approximately 0.61 g cm^{-3}, which is close to the values commonly observed in nano-scale materials.[S2,S3] As is depicted in Fig. S9, the N-C@SnO2-SnS/GN delivers initial discharge and charge specific volumetric capacities of 1202 and 796 mA h cm^{-3}, respectively, after 110 cycles, the electrode still retains a volumetric capacity of 734 mA h cm^{-3}. Such performance precedes graphitic anodes (~620 mA h cm^{-3}).[S4]

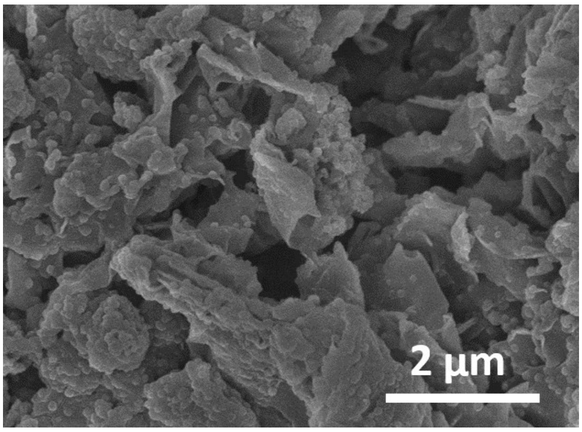

Fig. S10 SEM images of N-C@SnO_2-SnS/GN after cycling.

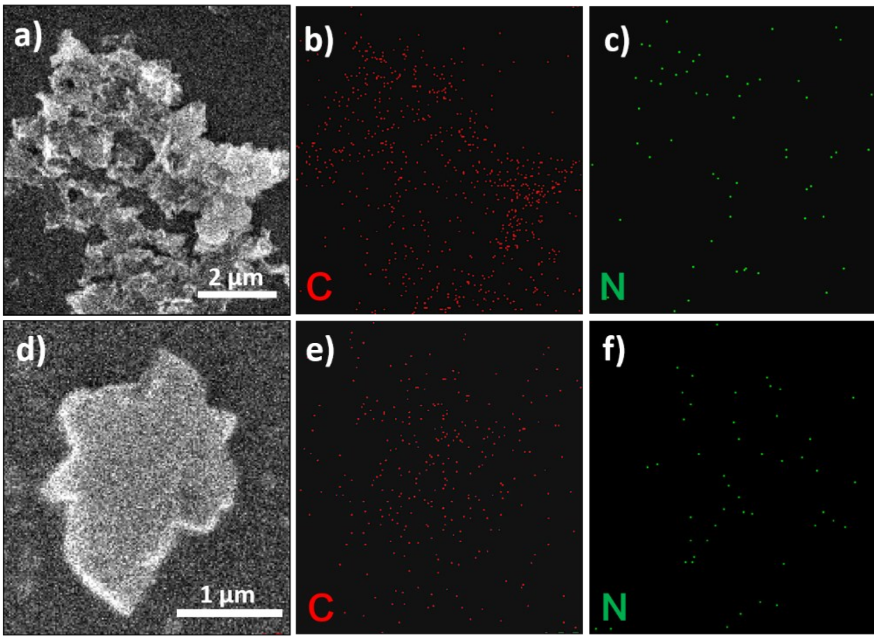

Fig. S11 SEM images of N-C@SnO_2-SnS/GN a) before and d) after cycling; b), e) corresponding elemental mapping images of C; c), f) corresponding elemental mapping images of N.

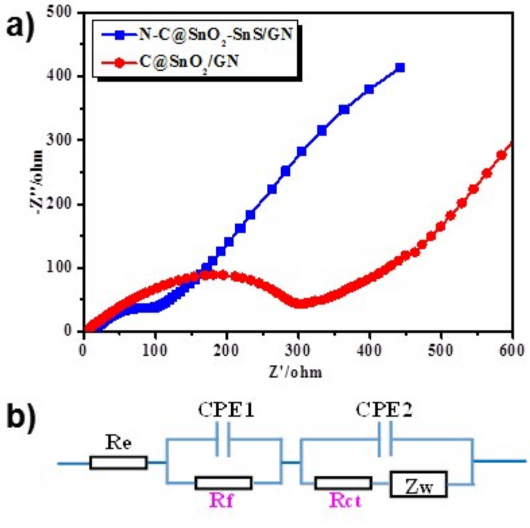

Fig. S12 a) Nyquist plots of N-C@SnO_2-SnS/GN and C@SnO_2/GN obtained by applying a sine wave with an amplitude of 5.0 mV over the frequency range 100 kHz to 0.01 Hz; b) Equivalent circuit model of the samples. R_e is the electrolyte resistance and R_f is the resistance of the surface film formed on the electrodes (contact resistance). R_{ct} is charge transfer resistance.

Table S1 Kinetic parameters of C@SnO_2/GN and N-C@SnO_2-SnS/GN.

Samples	C@SnO_2/GN	N-C@SnO_2-SnS/GN
$R_f(\Omega)$	44.64	17.69
$R_{ct}(\Omega)$	229	70.34

References:

S1 Y. Idota, T. Kubota, A. Matsufuji, Y. Maekawa and T. Miyasaka, *Science*, 1997, **276**, 1395-1397.

S2 S. W. Oh, S.-T Myung, H. J. Bang, C. S. Yoon, K. Amine and Y.-K. Sun, *Electrochemical and Solid-State Letters*, 2009, **12**, A181-A185.

S3 Y.-K. Sun, S.-M. Oh, H.-K. Park and B. Scrosati, *Adv. Mater.* 2011, **23**, 5050-5054.

S4 A. Magasinski, P. Dixon, B. Hertzberg, A.Kvit, J. Ayala and G. Yushin, *Nat. Mater.*, 2010, **9**, 353-358.